Hydrogen isotope geochemistry and heat balance of a fumarolic system: Kudriavy volcano, Kuriles

Roman E. Botcharnikov [a,*], Kirill I. Shmulovich [a], Sergey I. Tkachenko [a], Mikhail A. Korzhinsky [a], Alexander V. Rybin [b]

[a] *Institute of Experimental Mineralogy, Russian Academy of Sciences, 142432 Chernogolovka, Russia*
[b] *Institute of Marine Geology and Geophysics, Russian Academy of Sciences, 693008 Yužno-Sakhalinsk, Russia*

Abstract

The temperature and hydrogen isotope composition of the fumarolic gases have been studied at Kudriavy volcano, Kurile Islands, which is unique for investigating the processes of magma degassing because of the occurrence of numerous easily accessible fumaroles with a temperature range of 100–940°C. There are several local fumarolic fields with a total surface area of about 2600 m^2 within the flattened crater of 200×600 m. Each fumarolic field is characterized by the occurrence of high- and low-temperature fumaroles with high gas discharges and steaming areas with lower temperatures. We have studied the thermal budget of the Kudriavy fumarolic system on the basis of the quantitative dependences of the hydrogen isotope ratio (D/H) and tritium concentration on the temperature of fumarolic gases and compared them with the calculated heat balance of mixing between hot magmatic gas and cold meteoric water. Hydrogen isotope composition (δD and ^{3}H) shows a well expressed correlation with the gas temperature. Since D/H ratio and ^{3}H are good indicators of water sources in volcanic areas, it suggests that the thermal budget of the fumarolic system is mostly controlled by the admixing of meteoric waters to magmatic gases. The convective mechanism of heat transfer in the hydrothermal system governs the maximum temperatures of local fumaroles and fumarolic fields. Low-temperature fumaroles at Kudriavy are thermally buffered by the boiling processes of meteoric waters in the mixing zone at pressures of 3–12 bar. These values may correspond to the hydrostatic pressure of water columns about 30–120 m in height in the volcanic edifice and hence to the depth of a mixing/boiling zone. Conductive heat transfer is governed by conductive heat exchange between gases and country rocks and appears to be responsible for the temperature distribution around a local fumarolic vent. The temperature and pressure of shallow degassing magma are estimated to be 1050°C and 2–3 bar, respectively. The length of the 'main' fumarolic gas conduit is estimated to be about 80 m from the linear correlation between maximal temperatures of fumarolic fields and distances to the highest-temperature 'F-940' fumarole. This value may correspond to the depth of an apical part of the magmatic chamber. The geometry of the crater zone at the Kudriavy summit and the model of convective gas cooling suggest different hydrostatic pressures in the hydrothermal system at the base of high- and low-temperature gas conduits. The depths of gas sources for low-temperature fumaroles are evaluated to be about 200 m at the periphery of the magma chamber.
© 2003 Elsevier Science B.V. All rights reserved.

---

* Corresponding author. Present address: Institut für Mineralogie, Universität Hannover, Callinstr. 3, D-30167, Hannover, Germany. Fax: +49-511-762-3045.
  E-mail address: r.botcharnikov@mineralogie.uni-hannover.de (R.E. Botcharnikov).

1. Introduction

The temperature of volcanic gases is one of the main physical parameters of magma degassing and often shows a correlation with the stage of volcanic activity, gas emission rates and magma chamber depth (e.g., Giggenbach, 1987; Rowe et al., 1992; Connor et al., 1993; Stevenson, 1993; Symonds et al., 1996; Nuccio et al., 1999; Shinohara et al., 2002). In the case of shallow magma chambers or conduits, gases can flow through cracks directly open to the surface that impose minimal gas cooling. Therefore, temperatures of fumarolic gases are expected to be close to magma temperature. Low-temperature fumaroles, in turn, should be connected with deeper gas sources and/or gases should have undergone more effective cooling processes (Fischer et al., 1997). Although gas temperature is a function of magmatic system evolution (e.g., Symonds et al., 1996), the cooling of magmatic gases ascending to the surface, at a given moment, is mostly governed by the conductive heat transfer to country rocks and convective heat transfer in the hydrothermal system of the volcano.

A numerical model of fumarolic gas cooling as a result of conductive heat transfer to the gas conduit walls was developed by Connor et al. (1993). They showed that the gas temperature in the fumarole is mainly controlled by mass flow rates and noted that the response of gas temperatures to changes in mass flow is greatest in the fumaroles with low gas discharge and temperature. The results of numerical simulation of the conductive heat budget of a stationary fumarolic system for a wide range of possible depths of magmatic source, geometry of gas conduits, gas discharge rates, rock porosity and temperature gradients in surrounding rocks (linear conductive geotherm and 'hydrothermal' geotherm) revealed that the conductive gas cooling increases with a decrease in conduit diameter and gas discharge, and an increase in depth of magma and temperature gradient in rocks (Stevenson, 1993). The

effect of rock porosity is insignificant in steady-state conditions.

The most important result in Stevenson's model is the conclusion that the gas pressure at the base of gas conduits is a few times atmospheric only. This implies that most of the pressure drop occurs when gases escape from the magma and indicates that the vertical pressure gradient within the fumarole conduit is close to gasostatic. The idea of deficient gas pressure with respect to a hydrostatic gradient in surrounding rocks is also used in the models of vapor-dominated geothermal reservoirs (e.g., Truesdell and White, 1973). Furthermore, the pressure difference between gas conduits and water-saturated country rocks together with a hydrostatic pressure gradient can act as a 'pump', adding groundwaters to magmatic gases. On the way to the gas channels, groundwaters will be progressively heated up to boiling temperature, consuming a significant fraction of heat flow (e.g., Truesdell and White, 1973; Cathles, 1977; Hardee, 1982; Carrigan, 1986; Nuccio et al., 1999). In a region next to and above the boiling zone, superheated vapor will migrate upward, infiltrate into conduits and admix with magmatic gases. At constant overall permeability of the porous rocks, the depths of a gas source and a mixing zone are very important because they control pressure gradients between conduits and the hydrothermal system, and hence the mass flow of groundwaters.

Schematic physical-geochemical models of volcanic hydrothermal systems (e.g., Giggenbach, 1987; Giggenbach and Sheppard, 1989; Taran et al., 1992; Chiodini et al., 1993; Nuccio et al., 1999) and numerical simulation of groundwater circulation in a volcanic structure (Todesco, 1997) show that the ratio of magmatic and groundwater mass and heat flows is a very important factor controlling the distribution of isotherms in the volcanic edifice. Groundwater temperature variations in a 150-m-deep hole drilled 120 m from the active crater of Aso volcano, Japan, correlated with volcanic activity (Sudo and

Hurst, 1998). A horizontal fluid velocity approaching 200 m/yr was determined at Mount St. Helens, USA (Shevenell, 1991), indicating that groundwaters can flow significant distances in short periods through porous rocks. The continuous inflow of hydrothermal waters can lead to the formation of a water boiling zone, greatly buffering the temperature of fumarolic gas and evolving along a P–T boiling curve (Carrigan, 1986; Nuccio et al., 1999). Such a thermal buffering effect is probably the best explanation for the almost constant maximal gas temperature of about 315°C observed at Vulcano, Italy at the end of the 1970s and the beginning of the 1980s (Nuccio et al., 1999) and the occurrence of low-temperature boiling-point fumaroles at many other volcanoes.

Chemical (CO_2, CH_4, He, N_2, O_2, Ar, Cl) and isotope (D, ^3H, ^{13}C, ^{18}O, $^3He/^4He$, $^{220}Rn/^{222}Rn$) tracers are often used as indicators of mixing processes between magmatic gases and hydrothermal waters (Taran et al., 1992; Symonds et al., 1996; Tedesco and Scarsi, 1999; Nuccio et al., 1999; Goff and McMurtry, 2000; Capasso et al., 2000; Zimmer et al., 2000; Paonita et al., 2002). Moreover, the results of studies of CO_2, He and NaCl ratios in Vulcano fumarolic gases were used to create a model of the mixing processes accounting for mass and thermal budgets (Nuccio et al., 1999) which was further extended on the basis of H_2O and CO_2 isotope balance equations (Paonita et al., 2002).

Hydrogen and oxygen isotope ratios not only reflect the contribution of different sources to the composition of volcanic gases (O'Neil, 1986) but also show a correlation with the temperature of gases in many cases (e.g., Fischer et al., 1997; Goff and McMurtry, 2000). Such a correlation between temperature and isotope composition of fumarolic gases was already found in the first study on geochemistry of Kudriavy volcano gas jets (Tkachenko et al., 1992) and more recently by Taran et al. (1995) and Goff and McMurtry (2000). This was interpreted as a dilution and cooling of magmatic gases by meteoric waters. The heat exchange between gases and country rocks reduces gas temperature as well but the relationship of conductive and convective heat transfer in the volcano thermal budget has not been properly estimated to date. Several aspects are still not clearly understood: the contribution of meteoric waters to the gas composition of fumaroles with temperatures from 900 to 100°C; P–T conditions and the mechanism of mixing between groundwaters and gases; why fumaroles with a wide temperature range of more than 800°C are located on the same fumarolic field; in which manner the magmatic source is connected with the different fumarolic fields and what the possible depth of the magmatic source is.

To elucidate these issues, we compared the calculated heat balance of mixing between hot magmatic gas and cold meteoric water with a similar balance of isotope tracers. To do this, we studied the quantitative dependences of the hydrogen isotope ratio (D/H) and tritium content on the temperature of fumarolic gases. Estimations of geometry and characteristic sizes of fumarolic conduits were then made applying a simplified model of water filtration through the porous medium.

2. Kudriavy volcano

Kudriavy volcano (991 m elevation) is located in the northern part of Iturup Island, Kuril arc, Russia (Fig. 1a). The volcano is part of a post-caldera eruptive complex, consisting of the Medvezhy, Sredny, and Kudriavy, oriented along an NE–SW-trending line, and Men'shoi Brat volcanoes (Fig. 1b). Its last magmatic eruption with basaltic andesite lava flows occurred in 1883 (Gorshkov, 1970). The report of additional eruptive activity in 1946 documented by Simkin and Siebert (1994) was erroneous or there was a weak phreatic eruption because the ruins of Japanese mining are still in the crater. A recent phreatic eruption was observed on October 7, 1999 (Korzhinsky et al., 2002). The geological setting and rock compositions of Kudriavy volcano and Medvezhya caldera have been described in detail by Gorshkov (1970), Vlasov and Petrachenko (1971), Ermakov and Semakin (1996), Ermakov and Steinberg (1999), and Piskunov et al. (1999).

The total length of the Kudriavy summit is about 500–600 m with a width of 200–250 m
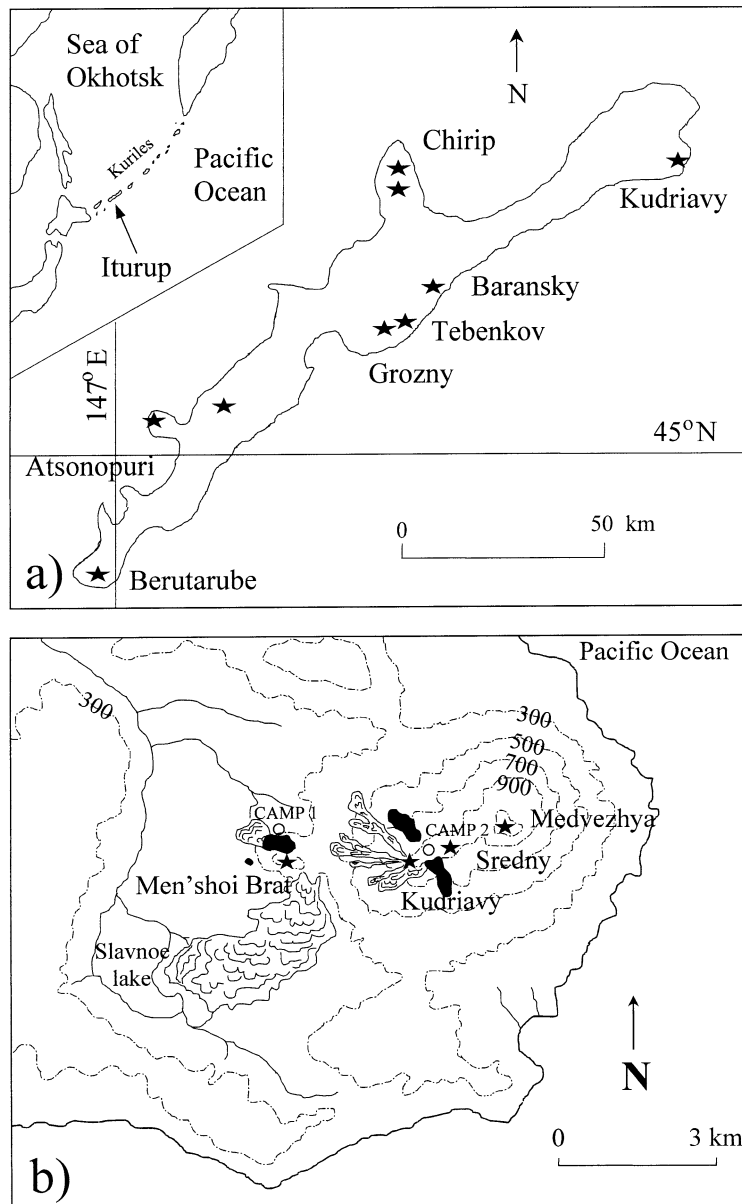
Fig. 1. (a) Location map of Kudriavy volcano in Iturup Island, Kuril arc. (b) Sketch map of the northeastern part of Iturup Island (contours every 200 m starting at 300 m elevation). Stars denote the positions of volcanoes, rhyolite domes are shown in black. Open circles are the camps at the base and at the summit of Kudriavy.

(Fig. 2). The volcanic slopes are composed of numerous basalt andesite lava flows, and pyroclastic debris and are mapped by Ermakov and Steinberg (1999). The top of the Kudriavy volcano consists of two cones: the eastern one is immediately adjacent to Sredny volcano and the western one is steeply sloping towards the Men'shoi Brat volcano (Fig. 1b). The eastern part is a flattened closed crater with an andesitic dome (about 20 m elevation) in the center (Fig. 2). The small crater (30 m in diameter and 25 m in depth) was formed just near the dome as a result of the last phreatic
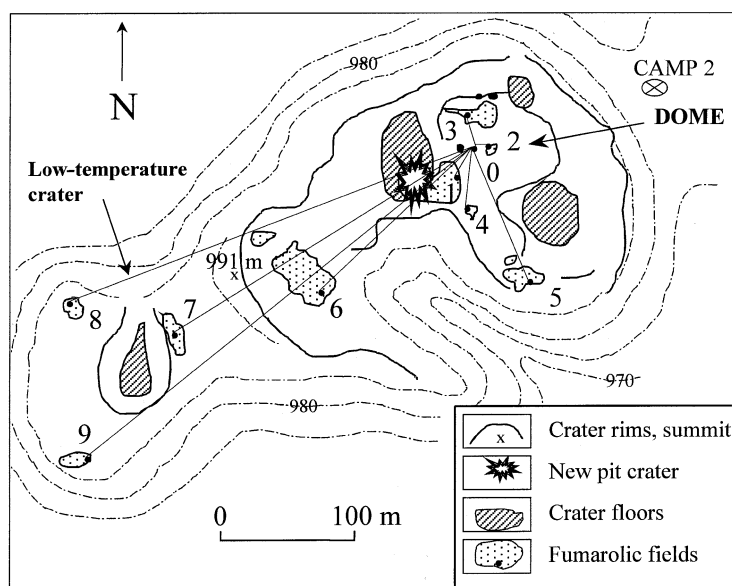
Fig. 2. The map of the crater zone at Kudriavy volcano. Big numbers denote the main fumarolic fields within the craters of Kudriavy and correspond to the numbers of fumarolic fields in Table 1. Solid lines are the distances from the highest-temperature fumarole 'F-940' to the fumaroles with maximum temperature at each fumarolic field (see also Fig. 3).

eruption in 1999. A second large explosive crater is located further to the west and is mostly filled with pyroclastic material. All lava flows from the last magmatic eruption are adjacent to the third crater located in the western part of the summit.

Kudriavy volcano is unique for investigating the processes of magma degassing because of the occurrence of numerous easily accessible fumaroles with a temperature range of 100–940°C at the top of a flattened cone (Fig. 2). There are several local fumarolic fields with a total surface area of about 2600 m^2. The highest-temperature fumaroles are distributed on the top and on the slopes of the dome in the eastern crater. These high-temperature fumarolic fields occupy the largest area at the summit and produce the largest emission of SO_2 flux (Fischer et al., 1998). Some fumaroles in these fields are characterized by outgassing velocities up to 120 m/s (Botcharnikov et al., 1998). Fumarolic fields of the second crater have medium temperatures (up to 630°C) and surface areas. Three low-temperature fumarolic fields with a total area of about 45 m^2 are located in the western crater.

An extensive volume of data on volcanic gas geochemistry was collected at Kudriavy on an annual basis from 1989 to 1999 (Tkachenko et al., 1992; Taran et al., 1995; Tkachenko, 1996; Wahrenberger, 1997; Fischer et al., 1998; Goff and McMurtry, 2000; Korzhinsky et al., 2002; Botcharnikov, 2002). Chemical and isotopic compositions of the Kudriavy volcano fumarolic gases are typical of arc volcanism (Giggenbach, 1992a,b). High temperatures of fumarolic gases, more than a 100-year period of intensive degassing and a 40–75-year age of admixing groundwaters (Goff and McMurtry, 2000) make it possible to suggest a quasi-steady-state degassing of shallow convecting magmatic melt in the volcanic edifice (Taran et al., 1995; Korzhinsky et al., 2002). However, the geometry and depth of the magmatic chamber are still unknown even after seismic and gravimetric measurements (Ermakov and Steinberg, 1999; Steinberg, personal communication, 2002). A compositional convection and degassing in a stratified magma chamber was proposed by Simakin and Botcharnikov (2001) as a possible mechanism for the continuous degassing

Table 1
Hydrogen isotope composition (δD, ‰ and ^3H, T.U.) of Kudriavy volcano fumarolic gas condensates sampled in 1990–1999

Number	Sample	Temperature (°C)	δD (‰) 1990–91	1993	1995	1999	^3H (T.U.)[c,d] 1995	Fumarolic field number or location
1	ZN1000[b]	932		−17				0
2	T926[b]	926		−21				0
3	TFC6–1[c]	920			−19			0
4	TFC6-2[c]	920			−22		0.06	0
5	B916[a]	916		−19				0
6	TK1391[b]	910	−12					0
7	B910-1[a]	910				−22		0
8	B910-2[a]	910				−23		0
9	B820[a]	820		−22				2
10	T810[b]	810		−21				2
11	ZN800[b]	800		−19				2
12	T735[b]	735		−20				3
13	B685[a]	685		−30				3
14	TFC8[c]	680			−40		0.59	3
15	T630[b]	630		−41				5
16	B620[a]	620		−24				5
17	TK291[b]	585	−23					5
18	B545[a]	545		−33				5
19	TK391[b]	542	−23					5
20	T538[b]	538		−29				5
21	K790[b]	511	−38					6
22	B474[a]	474		−27				6
23	T465[b]	465		−23				6
22	B450[a]	450		−26				6
24	K1190[b]	430	−26					6
25	ZN300[b]	300		−27				6
27	K990[b]	240	−32					7
28	TK2591[b]	187	−45					7
29	TFC10-1[c]	187			−51		2.45	7
30	TFC10-2[c]	187			−52			7
31	T170[b]	170		−54				7
32	B170[a]	170		−47				7
33	K690[b]	160	−49					8
34	TK1791[b]	130	−45					8
35	Warm spring[b]	39		−63				Caldera
36	Warm spring[c]	32			−64		9.4	Caldera
37	Rain-1[c]	14			−46		10.8	Caldera
38	Rain-2[c]	14			−47			

[a] This work.
[b] After Taran et al. (1995).
[c] After Goff and McMurtry (2000).
[d] T.U. = tritium units, where 1 T.U. = 1 ^3H atom in 10^{18} H atoms (Goff and McMurtry, 2000).

activity of the Kudriavy volcano. Alternatively, Fischer et al. (1998) have suggested that the long-term high-temperature degassing at Kudriavy is caused by a steady-state release of volatiles from the depth of arc magma generation and high heat flow from the mantle.

3. Field data

Measurements of physical parameters and gas sampling were repeatedly carried out on a long- and short-term basis at different fumaroles at Kudriavy during the last decade. The variations of
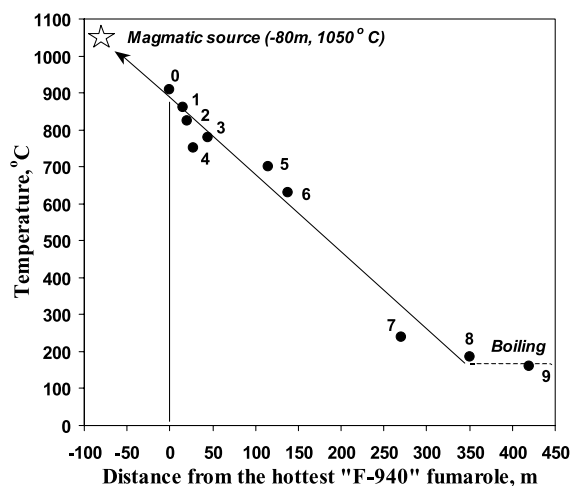
Fig. 3. The dependence of maximum temperature of fumarolic field on the distance from the highest-temperature 'F-940' fumarole. Note that distances are measured in different directions as shown in Fig. 2. Numbers correspond to the different fumarolic fields. The dashed line is for boiling temperatures of low-temperature fumaroles (see text). The extrapolation of the linear trend to 'negative distances' up to a temperature of 1050°C made it possible to estimate the depth of the magmatic gas source to be about 80 m. Star shows the temperature and depth of the magmatic source (see text for details).

magmatic gas temperature and composition in the highest-temperature fumarole 'F-940' have been discussed in detail by Korzhinsky et al. (2002). Here we summarize the data on gas temperatures and hydrogen isotope composition from different fumaroles and fumarolic fields located in the craters of Kudriavy volcano.

3.1. Fumarolic gas temperature

Temperature measurements are the most precise and can be performed with an error in accuracy of less than 1%. Chromel–alumel thermocouples, sheathed by a stainless steel capillary of 6 mm outer and 3 mm inner diameter, were used to measure the temperature of volcanic gases. Temperature measurements were conducted periodically at main fumarolic fields of Kudriavy between 1991 and 1999. Seasonal and weather temperature variations of high-discharge fumaroles at Kudriavy were within a range of ± 20°C. Korzhinsky et al. (2002) have reported that measurements at the highest-temperature fumarole 'F-940' showed a rapid temperature increase from 910°C in 1991 to 940°C in 1992 and then a small gradual temperature decrease from 940 to 907°C from
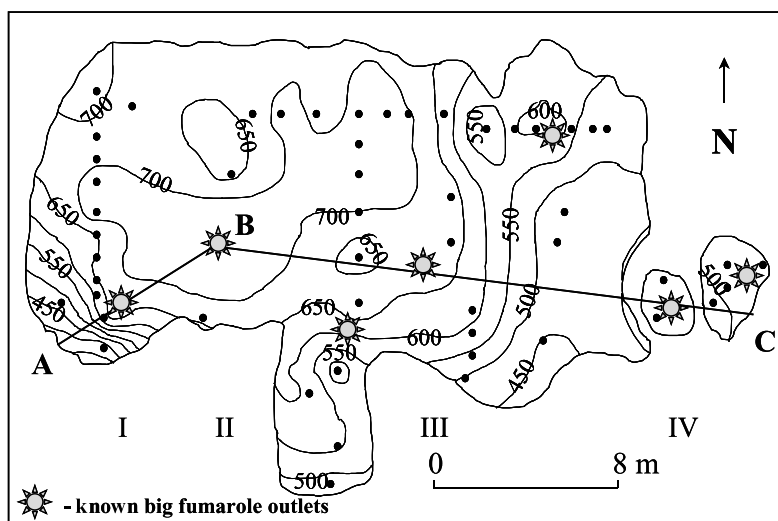

Fig. 4. Sketch map showing the distribution of temperature contours every 50°C (thin lines) on '605' fumarolic field (shown as number 5 in Fig. 2). Temperatures were measured at 20–30 cm depth after rock sample collection. Filled circles show the points of temperature measurements. Thick curved lines show the boundaries of the fumarolic field. Big stars are known fumaroles with high discharge rates. The straight solid line connecting points ABC is a temperature profile across the fumarolic field also shown in Fig. 12.

1992 to 1999. Other fumaroles are also characterized by almost constant temperature values during the last decade. Each gas sampling for isotope analysis was accompanied by a measurement of gas temperature (Table 1).

Fumaroles with a wide range of temperatures from the highest-temperature ones, with high discharge rates, to weakly steaming low-temperature ones are located almost at each fumarolic field. It must be noted, however, that maximal temperatures for each fumarolic field reveal a correlation with the distances from the highest-temperature 'F-940' fumarole (Fig. 3). The location of this 'main' hot fumarole was assumed as a zero reference distance while the distances to other fumaroles were measured in different directions as shown in Fig. 2.

The detail map of temperature contours at active fumarolic field '605' (number 5 in Figs. 2 and 3) of Kudriavy is shown in Fig. 4. Temperatures were measured during geochemical rock sampling of fumarolic fields at Kudriavy volcano in 1995. The measurements were performed at a depth of about 20–30 cm from the surface just after rock sample collection. Black solid circles in Fig. 4 correspond to points of rock sampling and temperature measurements. Big stars in Fig. 4 denote the locations of several known vigorous fumaroles within this field.

3.2. Hydrogen isotope composition of fumarolic gases

The fraction of magmatic water in volcanic gases may be determined from the ratios of stable isotopes of hydrogen and oxygen (e.g., Taran et al., 1995; Todesco, 1997; Goff and McMurtry, 2000). The isotopic composition of hydrogen in volcanic gases is more relevant for this purpose whereas oxygen isotopic composition may be changed by gas–rock interaction ('O-shift', e.g., Matsuo et al., 1974; Mizutani, 1978; Taran et al., 1995). Thus, in this study we have concentrated mostly on the behavior of hydrogen isotopes in fumarolic condensates.

The sampling procedure of gas condensates for isotopic analyses at Kudriavy has been described by Taran et al. (1995) and Goff and McMurtry

(2000). The data of this and previous studies on deuterium (δD, ‰) and the data of Goff and McMurtry (2000) on tritium (^{3}H, T.U.) isotopic compositions in fumarolic gases of Kudriavy volcano are presented in Table 1 and Fig. 5. All samples in Table 1 are separated by the date and place of sampling where the numbers of fumarolic fields relate to the numbers in Fig. 2. The various markers in Fig. 5 correspond to samples of different years. Circles denote the data obtained in 1990–91, squares represent the data of 1993, triangles denote the data of 1995, and crosses are the data of 1999. However, the temporal variations of δD composition in a single fumarole vent in 1991–1999 were studied only
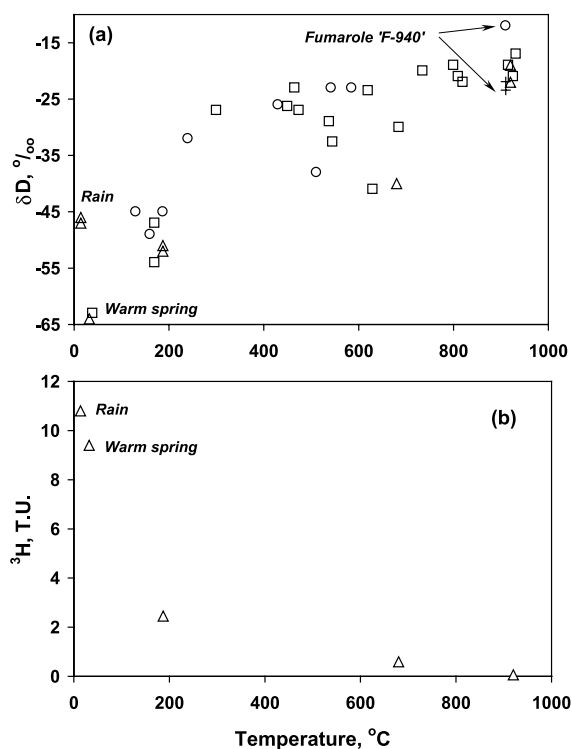

Fig. 5. Temperature dependence of hydrogen isotope composition in fumarolic gases of Kudriavy volcano: (a) deuterium, δD in ‰ and (b) tritium, ^{3}H in T.U. or tritium units (1 T.U. = 1 ^{3}H atom in 10^{18} H atoms). Circles denote the data obtained in 1990–91, squares correspond to the data of 1993, triangles denote the data of 1995, and crosses are the data of 1999 (see Table 1 for references). Two arrows show the range of D/H variations in the highest-temperature 'F-940' fumarole. The isotopic signatures for local rain and the warm spring are also plotted on both diagrams.
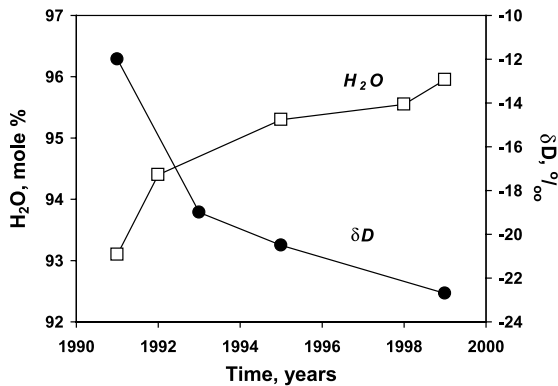
Fig. 6. Temporal variations of hydrogen isotope composition (δD) and H_2O concentration of the fumarolic gases periodically sampled from 'F-940' fumarole from 1991 to 1999 (average values for H_2O are calculated after Korzhinsky et al., 2002).

for fumarole 'F-940' (numbers 1–8 in Table 1) with $T > 900°C$ (average compositions for different years are shown in Fig. 6). The other fumaroles were not sampled repeatedly except two low-temperature fumaroles with $T = 187°C$ (numbers 28–30 in Table 1) and 170°C (numbers 31–32 in Table 1). Tritium concentrations in fumarolic gases were studied only in 1995 for the three fumaroles with different temperatures (Fig. 5b).

The deuterium compositions show a clear positive dependence on temperature (Fig. 5a) while the tritium content of fumarolic condensates correlates negatively with temperature (Fig. 5b). The waters of the warm spring inside Medvezhya caldera and local rains in 1995 are significantly enriched in tritium compared with the fumarolic gases.

4. Discussion

4.1. Hydrogen isotope composition of the meteoric and magmatic end-members

Taran et al. (1995) and Goff and McMurtry (2000) have pointed out that the fumarolic gases at Kudriavy are composed of a mixture of waters from magmatic and meteoric sources only. Their conclusion was drawn on the basis of δD vs. $\delta^{18}O$ and ^3H vs. $\delta^{18}O$ relations in gases shown in Fig. 7.

These relations resemble mixing trends from the high-temperature to the low-temperature samples and allow an evaluation of the isotopic compositions of the magmatic and meteoric end-members. It is clear that local rains cannot be the main source of meteoric waters admixing with magmatic gases because they are enriched in both deuterium and tritium relative to the low-temperature fumaroles (Figs. 5 and 7). The isotopic com-
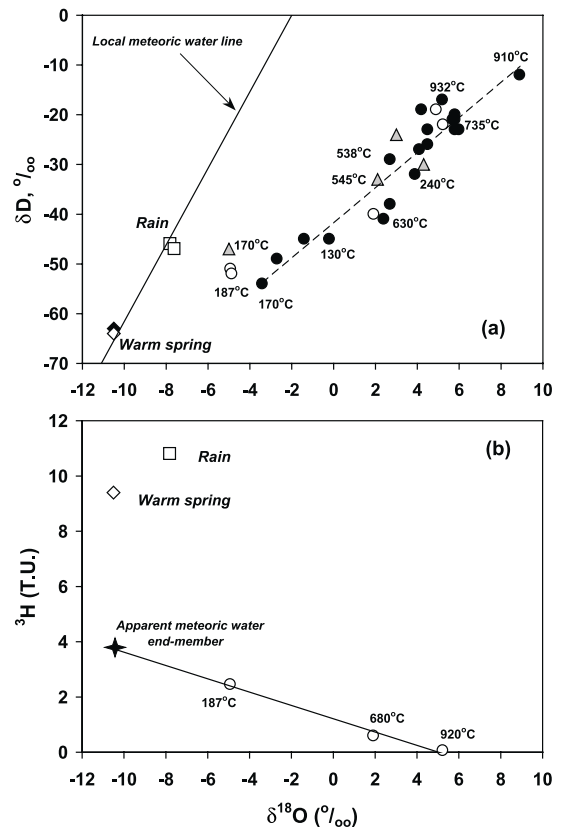

Fig. 7. The relationship between hydrogen and oxygen isotope compositions of the fumarolic gases (solid circles after Taran et al., 1995; open circles after Goff and McMurtry, 2000; triangles from this study), rains (squares after Goff and McMurtry, 2000) and warm spring (solid diamond after Taran et al., 1995; open diamond after Goff and McMurtry, 2000) at Kudriavy volcano. The D/H isotopic ratio shows a positive correlation with $\delta^{18}O$ in panel a, where the dashed line is a linear trend for the data of Taran et al. (1995). Tritium content correlates negatively with oxygen isotope composition (b). The extrapolated linear trend for tritium data points in panel b reaches the oxygen isotopic composition of the warm spring, which is assumed to be a meteoric end-member, at a value of about 4 T.U. (black star).

position of water in the warm spring is more relevant for the meteoric source at least for the deuterium data (Figs. 5a and 7a). The contrast in tritium contents between fumarolic gases and waters from the warm spring and rain (Figs. 5b and 7b) implies that the meteoric end-member of Kudriavy contains less ^3H than any modern meteoric water source and is about 40–75 years old (Goff and McMurtry, 2000). If we assume that meteoric water sampled in the warm spring is the meteoric end-member then we can estimate the apparent ^3H content in meteoric waters currently admixing with magmatic gases. Oxygen isotope composition of the meteoric waters should be relatively constant in time ($\delta^{18}O = -10.5\%$ in the warm spring). Therefore, extrapolation of the linear trend in fumarolic samples of the ^3H vs. $\delta^{18}O$ diagram (Fig. 7b) up to this constant value of the warm spring gives a tritium concentration in the apparent meteoric end-member of about $^3H = 4$ T.U.

It has been suggested that the high-temperature gases discharged from Kudriavy fumaroles display strong magmatic characteristics in both chemical and isotopic compositions (Taran et al., 1995; Fischer et al., 1998; Goff and McMurtry, 2000; Korzhinsky et al., 2002). Thus, we can suggest that the hydrogen isotope composition of fumarolic gases with temperatures above 900°C corresponds to the composition of pure magmatic gas at Kudriavy volcano which originated from 'andesitic waters' (Giggenbach, 1992a). However, as shown in Fig. 6, this magmatic end-member has been continuously depleted in deuterium from 1991 to 1999 whereas the amount of H_2O in the fumarolic gas continuously increased (average compositions after Korzhinsky et al., 2002). In this case we may expect one of two main processes affecting gas composition: a progressive dilution of initial magmatic gas by meteoric water or a continuous change in degassing conditions of a magma chamber.

A simple meteoric water dilution process will result in the continuous depletion in the high-temperature gas of the main magmatic components and D/H ratio. The δD vs. H_2O relation is shown in Fig. 8 for the three years (1991, 1995 and 1999) when fumarolic gases were sampled at 'F-940' fu-
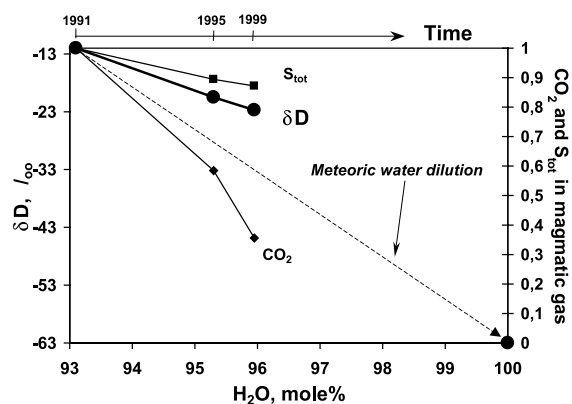

Fig. 8. The relationship between deuterium composition, relative concentrations of S_{tot} and CO_2 and water content of the highest-temperature fumarolic gases sampled in 1991, 1995 and 1999. The dashed line shows a trend of simple dilution of magmatic gas by meteoric water. The concentrations of sulfur and carbon dioxide have been assumed equal to 1 in 1991 and to 0 in pure water vapor.

marole for both chemical and isotopic analyses. The δD composition changes linearly with increasing water content in the high-temperature fumarolic gas, though showing a different behavior from the one that can be expected from simple dilution by meteoric waters (dashed line in Fig. 8). Fischer et al. (1998) revealed changes in chemical composition of parent magmatic gas at Kudriavy from 1992 to 1995. Further evolution of concentrations of major gas components in the parent gas was observed in 1998 and 1999 (Korzhinsky et al., 2002). Temporal changes in relative CO_2 and S_{tot} contents versus H_2O concentration in fumarolic gas from 'F-940' fumarole are plotted in Fig. 8 for comparison (average concentrations after Korzhinsky et al., 2002). The concentrations of those magmatic components were assumed to be equal to 1 in 1991 when sampling was started and 0 in pure water vapor. The amount of sulfur decreases linearly with increasing water content similar to δD but also more slowly than expected from simple meteoric water dilution. On the other hand, the carbon dioxide abundance in the magmatic end-member decreases much faster than deuterium and sulfur and even faster than meteoric water dilution. This means that the process of magmatic gas dilution by meteoric waters is not the main factor

controlling the temporal changes in composition of the magmatic end-member.

The continuous increase in H_2O concentration and decrease in δD, CO_2, and S_{tot} contents in fumarolic gases are likely to be directly related to degassing processes of Kudriavy magma and, moreover, to conditions of volatile release from an isolated magma volume (e.g., Giggenbach, 1996; Symonds et al., 1996). For gas exsolution close to the surface, open-system Rayleigh-type degassing will lead to continuous fumarolic gas depletion of deuterium (e.g., Matsuhisa, 1992; Shevenell and Goff, 2000) in accordance with hydrogen isotope fractionation coefficients between magmatic melt and fluid (Dobson et al., 1989; Pineau et al., 1998). However, the trend of hydrogen isotope changes in Fig. 6 does not correspond to the expected trend of deuterium depletion by Rayleigh-type fractionation. Note that the temperature of 'F-940' fumarole increased dramatically from 910°C in 1991 to 940°C in 1992 and then gradually decreased to 907°C in 1999 (Korzhinsky et al., 2002). Changes in chemical and isotope magmatic gas composition at Kudriavy since 1992 correlate well with a gradual temperature decrease from 940 to 907°C and may suggest an injection of a new, small, magma batch into a shallow magmatic chamber in 1992 and its further degassing (see also discussion by Korzhinsky et al. (2002)). In the case of a small magma batch injected into the magma chamber we can expect a rapid change in the 'new' magmatic gas composition gradually shifting to the gas composition of the 'old' magma. However, the lack of data before 1990 makes it impossible to unambiguously solve this problem. The fast change in CO_2 concentration and relatively slow changes in deuterium and sulfur contents shown in Fig. 8 probably result from the difference in distribution coefficients between magmatic melt and fluid phase for those components. Carbon dioxide has a much higher distribution coefficient than the other components resulting in rapid CO_2 depletion of the magmatic gas (e.g., Giggenbach, 1996; Dobson et al., 1989; Pineau et al., 1998).

Similar changes in chemical composition and hydrogen isotope ratio were found in samples from high-temperature A-1 fumarole at Showa-shinzan volcano collected during a 40-year period of volcano post-eruptive activity (e.g., Mizutani and Sigiura, 1982; Symonds et al., 1996). The decrease in fluctuations of hydrogen isotope composition with time was also shown at Showashinzan (Mizutani, 1978). The Rayleigh-type trend of deuterium depletion was observed at Mount St. Helens during the 1980–1994 period of magma degassing (Shevenell and Goff, 2000). In contrast, input of fresh magmatic material into the magmatic system led to an increase in the D/H ratio of magmatic gases as reported by Taran et al. (2001) for the new stage of Colima volcano eruptive activity.

Thus, we suggest that the magmatic end-member at Kudriavy is affected by continuous temporal variations mainly due to degassing processes in the magma chamber itself. The dilution effect of meteoric waters on the magmatic gas composition is supposed to have been relatively small during the last decade. Therefore, the absolute value of the D/H ratio in magmatic gas at Kudriavy changes with time but at each given moment reflects the isotopic composition of the parent magmatic gas and we can assume that the maximal D/H ratios for each year when samples were collected are close to the composition of magmatic gas. Goff and McMurtry (2000) estimated the tritium content of the Kudriavy magmatic end-member to be about $^3H = -0.32$ T.U. in 1995 and to date nothing is known about temporal variations of the tritium concentration.

4.2. T–δD and T–^3H correlation trends

Since fumarolic gases at Kudriavy volcano are a mixture of magmatic and meteoric waters only, the fraction of each constituent in gas samples can be evaluated from the simple equation:

$$X^m \cdot MAGM + MET \cdot (1 - X^m) = SAMP \qquad (1)$$

where X^m is the fraction of magmatic water in fumarolic gas, MAGM and MET denote hydrogen isotopic composition for pure magmatic gas and pure meteoric water, respectively, and SAMP is the isotopic composition of hydrogen for each sample. (The deuterium isotopic composition of meteoric water is assumed to be constant with

time ($\delta D = -63\%_o$, $X^m = 0$). The tritium concentration of meteoric water, determined as $^3H = 4$ T.U., is assumed to be the signature of meteoric end-member ($X^m = 0$) for fumarolic gas compositions in 1995. Although the magmatic water has a continuously changing δD composition, it is assumed to be representative of the magmatic end-member for each year of sampling ($X^m = 1$).) The magmatic signature for tritium is known only for 1995 and equals -0.32 T.U.

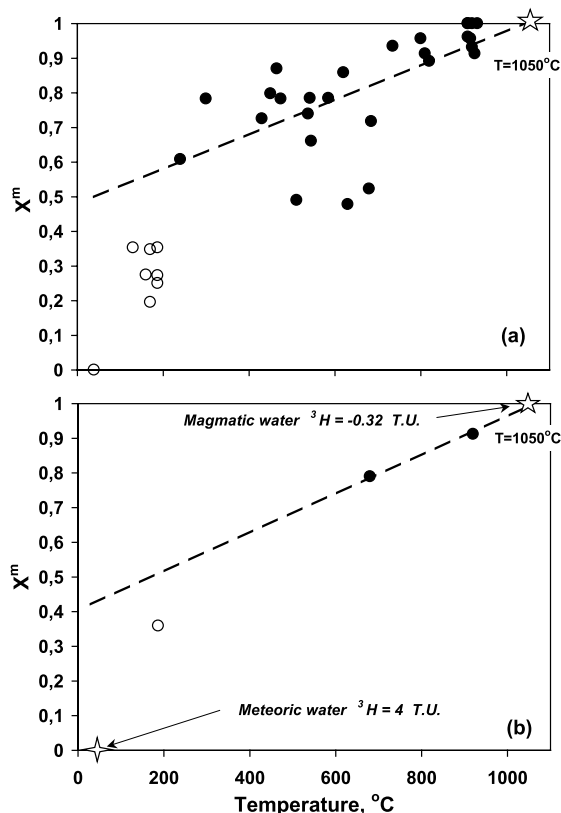The X^m deuterium values calculated in this way versus temperature are presented in Fig. 9a where

Fig. 9. Temperature dependence of magmatic water molar fraction calculated according to Eq. 1 (points) for the data on deuterium (a) and tritium (b) isotope compositions. Filled circles are the high-temperature gases, open circles denote low-temperature data. Dashed lines are linear trends for high-temperature points. The T–X^m linear trend of high-temperature samples in panel a achieves an X^m value equal to 1 at a temperature of 1050°C, which may correspond to the temperature of magmatic melt. Five-pointed stars show the magmatic end-member.

two series of data points can be clearly separated: samples with temperature >200°C (solid circles) and samples from low-temperature fumarolic fields ($T = 130–187$°C, open circles). The dashed line in Fig. 9a shows the T–X^m linear trend for high-temperature samples. The extrapolated linear trend of high-temperature points (dashed line) reaches the line of maximal D/H ratio ($X^m = 1$) at a temperature of about 1050°C (star in Fig. 9a). This temperature likely corresponds to the temperature of pure magmatic gas when it escapes from the magmatic melt and hence to the magma temperature. This value compares well with the estimated temperatures of andesitic magmas (e.g., Soufriere Hills volcano, Murphy et al., 1998; Unzen volcano, Venezhky and Rutherford, 1999; Ruapehu volcano, Nakagawa et al., 1999).

The X^m vs. T dependence calculated for tritium compositions is shown in Fig. 9b. The temperature of the magmatic end-member is assumed to be 1050°C and its tritium content (-0.32 T.U.) is after Goff and McMurtry (2000). The dashed line again shows the linear trend for the three high-temperature points. The slopes of the linear trends are almost identical for deuterium and tritium data points, suggesting a similar temperature dependence for the two hydrogen isotopes.

The observed wide variations in D/H values may be caused by many factors. The precision of δD measurements is usually $\pm 1\%_o$ while analytical dispersion in different laboratories may increase this value by a factor of 2. The additional error may result from hydrogen isotope fractionation through condensation/evaporation during sampling with temperature dependence on not only the value, but also the sign of fractionation. The gas phase is 'lighter' in deuterium in relation to liquid at temperatures <250°C, and 'heavier' in deuterium at temperatures >250°C (O'Neil, 1986). Therefore, the isotopic composition of some condensate samples from high-temperature fumaroles may be enriched in deuterium due to partial evaporation during sampling. It is also evident from Fig. 9a that several 'high-temperature' points have low X^m, i.e., δD values. Such sample depletion in deuterium may be expected from evaporation at $T>250$°C, however it is not possible according to the sampling procedure

and sample conservation (Taran et al., 1995; Goff and McMurtry, 2000).

One mechanism explaining the observed shift of 'middle-temperature' points from the $T–X^m$ trend in deuterium depletion in Fig. 9a may be an excess heating of gases enriched in meteoric component. High-discharge-rate fumaroles can heat the surrounding rocks and low-discharge gas jets. If sampling is conducted in such a low-discharge-rate but 'overheated' fumarole then sample is expected to be depleted of deuterium in relation to the $T–X^m$ trend. Also, a portion of meteoric water flow may be heated up and boiled by the magmatic chamber itself. Then, these hot meteoric vapors can mix with magmatic gases in the fumarolic conduits, preserving low D/H ratios and high gas temperatures.

Another mechanism is more hypothetical. Twenty-day continuous monitoring of the high-temperature Kudriavy fumaroles revealed a dramatic increase in H_2 concentration from 1–1.3 up to 10 mol% in fumarolic gases during 5 days in 1998. Elevated hydrogen contents up to 5 mol% in gases were also observed after the phreatic eruption in 1999 (Korzhinsky et al., 2000). These observations suggest a cause of significant variations in D/H ratio. The difference between δD values in water vapor and hydrogen of fumarolic gases (Mizutani and Sigiura, 1982) and in the $H_2O–H_2$ system (Richet et al., 1977) is about 200‰ at temperatures around 600°C. This means that H_2 is highly depleted of deuterium in relation to H_2O. An admixing of this hydrogen to fumarolic gases following its oxidization to H_2O and the accompanying reduction of SO_2 to H_2S adds 'light' water to the system. A possible great influence of deuterium exchange in the $H_2O–H_2S–H_2–HCl–HF$ gas system on the D/H ratio of fumarolic gas was also discussed by Chiodini et al. (2000). However, it is difficult to quantitatively determine this effect of the exchange reactions among gas components.

It must also be noted that the processes of isotope fractionation from meteoric water boiling/condensation around the gas conduits are likely to have no effect on isotopic composition of fumarolic gases. The stability of fumarolic temperatures at Kudriavy volcano during a long period

suggests almost isothermal conditions of magma degassing, quasi-steady-state conditions of heat and mass transfer in the volcano edifice, and hence a continuity of magmatic and meteoric water flows. In this case, the hydrogen isotope composition of both meteoric water and magmatic gas entering the zone of mixing is constant.

Since the temperatures of high-temperature fumarolic gases correlate well with their isotopic composition, we suggest that the process of mixing between magmatic and meteoric waters plays a very important role in the thermal budget of the fumarolic system at Kudriavy.

4.3. Heat balance of mixing between magmatic gases and meteoric waters

The heat balance of mixing, between cold meteoric water and hot magmatic gas, can be easily calculated. Since fumarolic gases at Kudriavy volcano consist mainly of water vapor (93–98 mol%; Taran et al., 1995; Wahrenberger, 1997; Fischer et al., 1998; Korzhinsky et al., 2002), a mixing relationship can be considered for cold water ($T = 20°C$) and high-temperature water vapor. We calculated the enthalpies of mixing at various ratios (molar fractions) of these components taking into account an additivity of enthalpies and
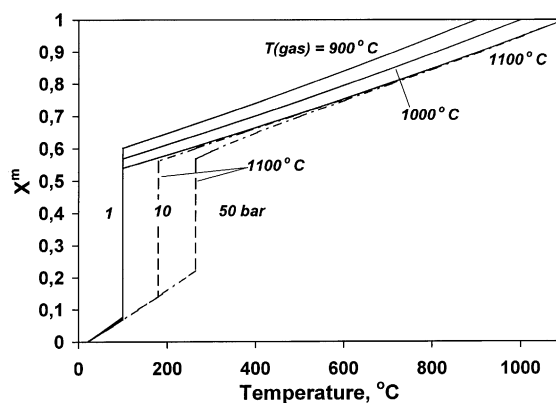

Fig. 10. Temperature dependence of mixing between hot magmatic gas and cold meteoric water (calculated by Eq. 2). Solid lines show the temperature dependence of the molar fraction of magmatic water in the mixture at different initial temperatures (900–1100°C and $P = 1$ bar) of magmatic gas. Dashed lines denote mixing relationships at pressures of 10 and 50 bar and a temperature of 1100°C.

specific enthalpy of vaporization/condensation. The calculation procedure can be expressed by the following equation:

$$H^{m} \cdot X^{m} + H^{met} \cdot (1 - X^{m}) = H^{mixt} \qquad (2)$$

where H^{m}, H^{met}, and H^{mixt} are the specific enthalpies (kJ/mol) of hot water vapor (magmatic gas), cold meteoric water, and the resulting mixture, respectively; X^{m} denotes the molar fraction of magmatic gas in the mixture. Further, the obtained enthalpy values (H^{mixt}) allow determination of the temperatures of mixture for both liquid and vapor from the data set. The data from the steam tables of Haar et al. (1984) were used.

The mixing proportions between hot magmatic vapor and cold water, calculated as a function of temperature and pressure, are plotted in Fig. 10. The calculations were conducted for initial temperatures of magmatic gas in the range of 900–1100°C considering mixing $P = 1$ bar and for mixing pressures of 10 and 50 bar at $T = 1100$°C. Vertical lines on the diagram correspond to the liquid–vapor phase transition at different pressures. The data show that magmatic gas can be cooled down 1000°C (from 1100 to 100°C, $P = 1$ bar) when diluted less than 50% by meteoric water (at admixing of approximately 46% meteoric water).

The variations in the initial temperatures of magmatic gas also slightly affect the resulting temperature of mixture. With a magma temperature decrease of 200°C (from 1100 to 900°C, $P = 1$ bar), the ratio of components changes by 0.04 X^{m} (10 relative %) at water-saturated conditions. A pressure increase yields almost no effect on component ratios in liquid and vapor phases (Fig. 10) but leads to an increase in the temperature of vaporization/condensation, in accordance with P–T conditions of water saturation.

These calculated proportions of magmatic gas–meteoric water mixing can be compared with the temperature dependence of δD and ^{3}H measured in fumarolic gases of Kudriavy (Fig. 9). Since the T–X^{m} trend of isotopic data points in Fig. 7 allowed an evaluation of the magma temperature of about 1050°C, the calculated temperature dependence of gas–water mixing was found to be in accordance with Eq. 2, assuming the temperature

of magmatic gas is also equal to 1050°C at pressures of 1, 10, and 50 bar. The results are shown as solid lines in Fig. 11. As can be seen from the diagrams, isotope compositions are in good agreement with the calculated trends of the magmatic gas–meteoric water mixing relationship (dashed lines), even at temperatures < 200°C. The temperature trend for tritium gas composition lies a bit lower than the calculated trend of mixing between meteoric and magmatic water (Fig. 11b) but there are only a few points and large uncertainties in determination of 'tritium' end-members.
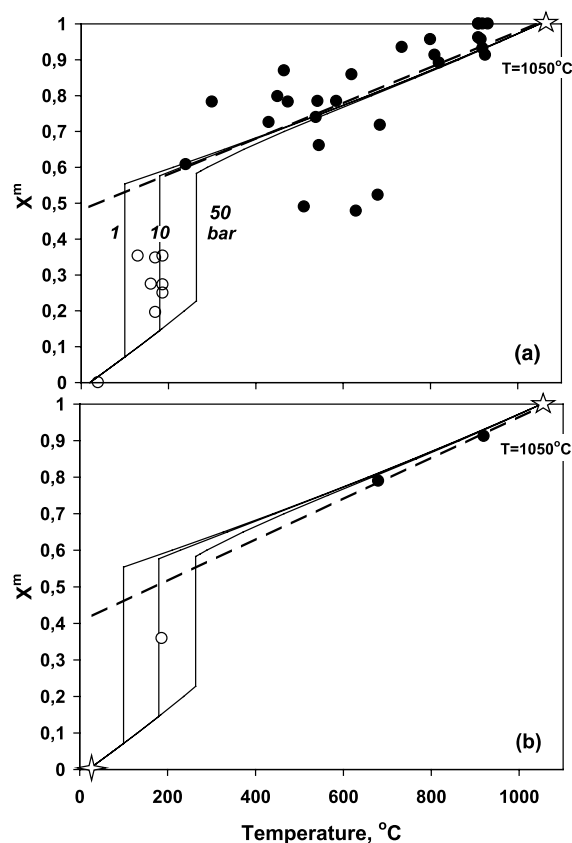

Fig. 11. Comparison of the magmatic water fraction in fumarolic gases vs. temperature derived from hydrogen isotope compositions (points in panel a from deuterium data and in panel b from tritium data, Eq. 1) and calculated from the heat and mass balance at mixing of hot magmatic gas and cold meteoric water $T = 1050$°C and $P = 1$, 10 and 50 bar (solid lines, Eq. 2). Filled circles are the high-temperature samples and open circles are low-temperature ones. Five-pointed stars are magmatic water and four-pointed star in panel b corresponds to meteoric water.

The low-temperature points in Fig. 11 lie on the calculated lines of meteoric water boiling in the temperature range of 130–187°C. These boiling temperatures correspond to pressures of about 3–12 bar. As mentioned above, the pressure gradient between gas channels and water-saturated country rocks is controlled by the boundary conditions: gasostatic pressure in the gas channels and hydrostatic pressure in rocks. Since the gasostatic pressure is low, the pressure gradient will be governed mostly by the hydrostatic pressures of meteoric waters. If the zone of meteoric water boiling and mixing is localized at some depth in the volcano structure then these values may reflect the hydrostatic pressures of water columns about 30–120 m in height from the level of underground waters and hence the depths of the mixing/boiling zone. At a high rate of meteoric water inflow into gas conduits, they can buffer the surface emission temperature of fumarolic gases at the level corresponding to P–T conditions of the boiling/mixing zone (Nuccio et al., 1999). In contrast, if this zone is distributed along all the length of fumarolic conduits then those pressure values will correspond to some average pressures of meteoric water boiling and admixing.

It must also be noted that the level of underground waters is not constant due to the high porosity of friable crater material and the high intensity of meteoric precipitation on the Kuril Islands. The variations in precipitation intensity lead to pressure fluctuations in the zone of meteoric water filtration and hence to variations in the magmatic/meteoric water ratio. Therefore, gas samples collected on different dates may have different isotopic D/H compositions while fumarolic temperature variations may be delayed due to the heat capacity of country rocks. This means that the intensity of meteoric precipitation may be an additional explanation for possible variations in isotopic gas composition discussed earlier.

The close correlation between the calculated temperature dependence of magmatic gas–meteoric water mixing and the data derived from hydrogen isotope composition of fumarolic gases suggests that the admixing of meteoric waters is a dominant mechanism governing the thermal budget of the fumarolic system at Kudriavy volcano.

4.4. Conductive heat transfer

Conductive heat transfer is also very important in volcanic areas. McGetchin and Chouet (1979), for instance, have reported that "aside from convection, conduction accounts for the order of 84% of the total energy balance" of Stromboli volcano. The contribution of conductive heat transfer in the fumarolic system of Kudriavy can be exemplified by the following observations.

The map of temperature contours at active fumarolic field '605' of Kudriavy is shown in Fig. 4. The temperature profile along line ABC (Fig. 4) is plotted in Fig. 12. The temperature peaks (I–IV) in Fig. 12 are related to four local fumarole outlets within the fumarolic field. A steep slope of the left part of peak I apparently shows a sharp temperature gradient between separate fumarolic vents on the edge of the fumarolic field and surrounding rocks. The calculated temperature distributions in a medium (rocks) with conductive cooling of a cylindrical pipe (gas conduit) are shown as dashed lines in the inset of Fig. 12. Calculations were performed with the help of a simplified equation, taking no account of heat losses from the surface and of physical properties of the surrounding rocks (e.g., Isachenko et al., 1969):
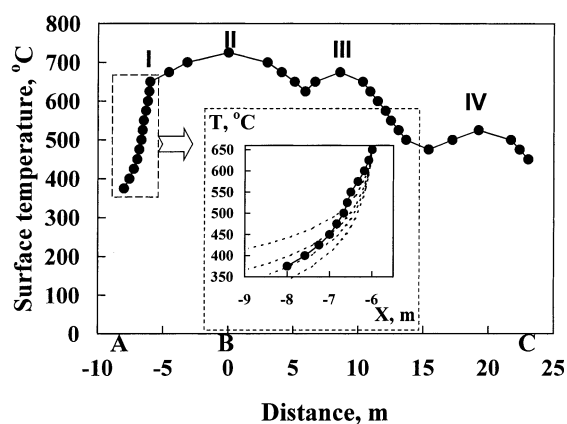

Fig. 12. The temperature distribution at '605' fumarolic field along line ABC as shown in Fig. 4. Peaks I–IV represent the local fumarole outlets. The inset shows temperature distribution in rocks (dashed lines) at conductive cooling of the gas conduit calculated by Eq. 3 and temperature distribution of peak I.

$$T_r = T_0 - (T_0 - T_\infty)\ln\left(\frac{r}{r_0}\right)/\ln\left(\frac{r_\infty}{r_0}\right) \qquad (3)$$

where T_r (°C) is the temperature of the medium at distance r (m) from the gas conduit, T_0 (°C) represents the temperature of gas and conduit wall, r_∞ (m) denotes the distance from the conduit where the temperature T_∞ (°C) is equal to the ambient temperature of 20°C, and r_0 (m) is the conduit radius. The initial temperature of gas and conduit wall was assumed to be 650°C, corresponding to the maximum temperature of peak I while the conduit radius was assumed to be 0.1 m. The different temperature profiles correspond to distances $r_\infty = 50$, 100, 200, and 1000 m from the conduit to the point of ambient temperature and hence to different temperature gradients in country rocks. As can be seen from the diagram, the shape of the temperature profiles for the calculated conductive heat transfer agrees in a first approximation with the shape of the temperature profile of peak I. This implies that conductive heat transfer can be responsible for the distribution of isotherms just around the local fumarole. In this case, the temperature gradients in country rocks can reach values of about 140°C/m or even higher (see Fig. 12).

In contrast, the temperature distribution within the fumarolic field is characterized by rather smooth temperature variations with the average temperature gradient along profile BC being about 10°C/m (Fig. 12). Local fumaroles thermally interact with each other inside the fumarolic area due to convective heat exchange, controlling the distribution of temperatures within the local fumarolic field. In addition, there are low-discharge gas jets around the fumaroles that also affect temperature distribution. These facts imply that sufficient interference of heat fields of the fumaroles may be expected within the local fumarolic area. This can lead to possible variations in the T–D/H relationship in low-discharge-rate fumaroles because of the excess heating by neighboring high-discharge vents. Such a mechanism of heat exchange among different fumaroles, along with those mentioned above, can partially explain the wide variation of points in Figs. 9a and 11a.

Thus, conductive heat transfer from gas con-duits, discussed in detail by Stevenson (1993) and Connor et al. (1993), appears to be a minor factor of the thermal budget, governing the temperature distribution only around local fumarolic vents, whereas convective heat transfer in the hydrothermal system controls the maximum temperatures of local fumaroles and the temperature distribution inside the fumarolic fields.

4.5. Other mechanisms controlling gas temperature

As discussed above, the temperature regime of fumaroles is mostly controlled by the heat exchange of fumarolic gases with the hydrothermal system and country rocks. However, apart from the heat exchange, gas temperature measured in the surface fumaroles may also be dependent on two additional processes in the gas phase itself. The first process is gas cooling due to adiabatic expansion as gases ascend from the magmatic chamber to the surface while the second is gas heating due to exothermic reactions of gas oxidation when gases interact with air.

The temperature change due to adiabatic expansion is thoroughly described in standard thermodynamics texts (e.g., Vukalovich and Novikov, 1972). There are two idealized end conditions of this process: (1) a completely reversible adiabatic gas expansion and (2) a completely irreversible expansion.

(1) The simple example of a reversible adiabatic process is gas expansion by slow pulling of a frictionless piston out of a cylinder. The amount of gas cooling in this process can be estimated from the Poisson equation:

$$T_f = T_i \left/ \left(\frac{P_i}{P_f}\right)^{\frac{\chi-1}{\chi}} \right. \qquad (4)$$

where T_i, T_f, P_i, and P_f are temperatures and pressures at initial and final conditions, respectively; $\chi = C_p/C_v$ is the ratio of gas heat capacity at constant pressure and volume. In this case, temperature drop may be significant. If $T_i = 1100$°C then a decrease in pressure from $P_i = 10$ bar to $P_f = 1$ bar will result in a temperature decrease to $T_f = 630$°C.

(2) Irreversible adiabatic gas expansion is anal-

ogous to the process of rapid gas decompression from a chamber to a vacuum. In practice, this effect may be recognized when gases flow through a valve with small perforations or a porous partition (Joule–Thomson effect). The gas enthalpy during the expansion process remains constant, as the work done by the expanding gas is almost balanced by the work done during gas forcing through the porous partition. If the pressure difference is small then the change in gas temperature through adiabatic expansion may be estimated from the equation (e.g., Vukalovich and Novikov, 1972):

$$T_f - T_i = \alpha(P_f - P_i) \tag{5}$$

where T_i, T_f, P_i, and P_f are initial and final gas temperature (K) and pressure (bar), respectively; α denotes the Joule–Thomson coefficient (K/bar). The extrapolation of data of Haar et al. (1984) on α temperature dependence of water vapor to temperatures of 1000–1100°C at low pressures gives a value of about 0.12 K/bar. Thus, the temperature decrease during irreversible adiabatic gas expansion, for instance, from 10 to 1 bar, is estimated to be about 1–2°C.

It is expected that the Joule–Thomson mechanism of gas expansion is more relevant at depth, where rock permeability is low. At shallow depths, within the last 500 m, rock permeability can be increased by a factor of 1000 (Criss and Taylor, 1986), which leads to a shift of gas expansion conditions toward the first case of adiabatic expansion (as suggested by Nuccio et al., 1999). This effect may be well expressed in volcanic environments where fractured old magma channels exist.

Since the permeability of rocks is expected to be relatively high in the Kudriavy edifice, the adiabatic gas expansion should be very efficient. As we measured surface fumarolic temperatures up to 940°C, we assume a low pressure gradient between the magmatic source and surface. The analysis of Eq. 4 implies that the pressure above the magma at a temperature of 1050°C will be equal to only 2–3 bar. This conclusion agrees well with the results of the numerical simulation of fumarolic gas flows conducted by Stevenson (1993).

The elevated temperatures of volcanic gases in relation to magmatic melt were measured, for instance, at Erta'Ale and Niragongo lava lakes. Temperature measurements of the magma and releasing gases revealed differences of 100–260°C (e.g., Le Guern et al., 1979; Le Guern, 1987). The increase in gas temperatures was due to involvement of air and exothermic oxidation of gas components. However, analyses of fumarolic gas chemical compositions at Kudriavy showed low concentrations of N_2 and Ar and hence insignificant air contamination (Taran et al., 1995; Wahrenberger, 1997; Fischer et al., 1998; Korzhinsky et al., 2002). Thus, the effect of oxidizing reactions may be eliminated.

4.6. Geometry of gas conduits

Fumaroles with a wide temperature range are located in each fumarolic field but maximal temperatures of the fumarolic areas revealed a correlation with the distance from the highest-temperature 'F-940' fumarole (Fig. 3). The location of the 'main' hot fumarole was assumed as a zero reference distance while the distances to other fumarolic fields were measured in different directions as shown in Fig. 2. The apparent linear dependence allows one to make some suggestions about the geometry of the magmatic gas source and gas conduits assuming the mixing relationship
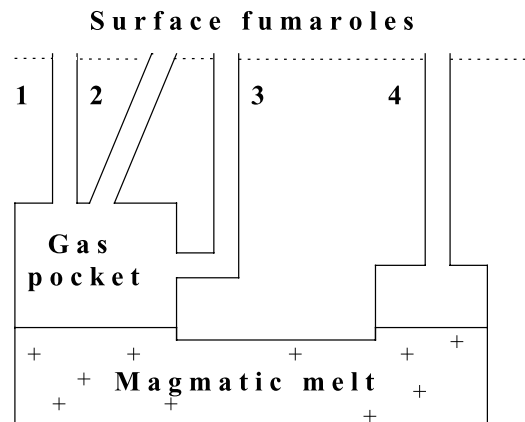

Fig. 13. Schematic geometry of gas conduits and magmatic chamber. The relationship among different gas conduits 1–4 is discussed in the text.

of magmatic gases and meteoric waters as a dominant mechanism of the thermal budget of the fumarolic system.

The possible geometry of gas conduits connecting the magmatic gas source with the surface fumaroles is shown schematically in Fig. 13. Case 1 corresponds to a gas conduit supposed for the 'main' fumarole where admixing of meteoric water is minimal or absent. Case 2 differs from case 1 only in length whereas case 3 is analogous to case 2 but with a different depth of the magmatic gas source. Case 4 is supposed for a magmatic chamber separated as several apophyses with different depth, mass of magmatic melt and degassing kinetics. If model 4 is realized at Kudriavy then the linear dependence in Fig. 3 may appear only occasionally while a regular increase in meteoric water content with increasing distance from the 'main' fumarole requires a rather special structure of magma apophyses.

The simpler model of a single source of magmatic gas is likely to be a more appropriate explanation of the observed regularity. The surrounding rocks may be considered as a porous isotropic medium where filtration of meteoric waters is governed by Darcy's law. This means that rock permeability is relatively constant and the involvement of meteoric waters in gas conduits, approximated as hypothetical 'tubes', is dependent upon the hydrostatic pressure (P_h) and the total surface area of the 'tube' walls. *Other factors being equal*, the total surface area of the 'tube' is proportional to its diameter and length.

In the case of diameter increase at constant length, the 'tube' cross-section will increase more rapidly than its surface area. Thus, the discharge of magmatic gas will increase more rapidly than the quantity of admixing meteoric water. Therefore, higher temperatures may be expected at fumaroles with larger diameters. If this takes place then the regular decrease in diameter of gas conduits from the central crater to the periphery will lead to a regular decrease in fumarolic temperatures. However, such a suggestion would be appropriate only for a volcanic structure with a regular radial distribution of fissures, for instance, for a single explosive crater. The summit of Kudriavy volcano consists of at least three overlaid

craters of different age (see Fig. 2), therefore the single-fissure structure is unlikely.

On the other hand, if we make a rough assumption that the diameters of all hypothetical 'tubes' are rather equal, then the 'tube' surface area will be proportional only to its length. In this case, the difference in meteoric water influx and hence in fumarolic temperatures for 'tubes' 1 and 2 is a function of conduit length. For a single gas source in model 1-2, this function may be considered linear to a first approximation. Then, we suggest that the extrapolation of linear temperature dependence in Fig. 3 to 'negative distances' corresponds to motion from the 'main' fumarole outlet to the magmatic chamber. A temperature of 1050°C, which was assumed from isotopic data as the magmatic temperature (Fig. 9), is achieved at a depth of about −80 m (see Fig. 3 for details). This would suggest a very shallow magma at a depth of about 100–150 m under the central crater if a volume of a possible gas pocket in the apical part of the magma chamber is taken into account. It must also be noted that these values are in good agreement with the independent estimations of the depth of the mixing zone between magmatic gases and meteoric waters obtained above. Similar estimations of the depth of the apical part of the magmatic chamber have been done by Ohminato and Erditato (1997) at Satsuma Iwojima volcano, Japan, which is also characterized by long-term (500–600 years) and high-temperature ($T \leq$ 870°C) fumarolic activity (Shinohara et al., 1993, 2002). Geophysical studies revealed the source of low-frequency earthquakes at a depth of about 40 m just under the Satsuma Iwojima volcano crater which was interpreted as a result of active degassing processes (Ohminato and Erditato, 1997).

The model of gas conduit geometry according to type 1-2 explains the linear dependence of temperature on distance from the 'main' fumarole but is in poor agreement with the observations on a quantitative basis. The length of hypothetical 'tubes' increases more slowly than would be expected from the degree of gas–water mixing at a given temperature. Analysis of the diagrams in Fig. 11 shows that the quantity of meteoric water in fumaroles with temperatures of 900°C may be up to 10%, whereas in low-temperature fumaroles

with temperature of 200°C it may reach 40%. If one recalculates the above values to 1 kg of magmatic gas they can be estimated as about 111 and 666 g of meteoric water, respectively. This means that the contribution of meteoric water to low-temperature fumaroles is six times greater than to high-temperature ones and, assuming that the proportion of meteoric water is solely dependent on conduit length, the length of the low-temperature gas conduit will be: $80 \times 6 = 480$ m. Obviously, at the single gas source and with the horizontal distance from the 'main' to the low-temperature fumarole equal to 270 m (Fig. 2), this value is almost two times more than that obtained from the simple geometric considerations.

The model of type 1-3 seems more relevant in this sense because with an increase in gas source depth, the hydrostatic pressure of admixing meteoric waters also increases. This increase in P_h will lead to a further increase in mass flow and intensity of meteoric water influx into gas conduits. In this case, the integral mass flow of meteoric waters, depending not only on conduit length but also on hydrostatic pressure at all levels, must be taken into account for the same magmatic gas–meteoric water ratios in high- and low-temperature fumaroles. In the simplified case, the mass flow (J) is directly proportional to hydrostatic pressure ($P_h = \rho \cdot g \cdot H$; since gas pressure is very low inside fumarolic conduits) and the total surface of the gas conduit or, at constant diameter, to its length (H):

$$J \approx P_h \cdot H \approx \int_{H_0}^{H_1} \rho \cdot g \cdot H \, \mathrm{d}H \approx H^2/2$$
$$(\text{if } \rho \cdot g = \text{const}) \tag{6}$$

where ρ is water density and g is acceleration due to gravity. Then, this dependence of meteoric water mass flow on the length of gas conduits allows an estimation of the possible depth of a low-temperature fumarole source to a first approximation. The ratio of meteoric water in high- and low-temperature fumaroles as $1 \div 6$ gives:

$$6 \cdot H_1^2/2 = H_2^2/2 \tag{7}$$

where $H_1 = 80$ m is the length of the 'F-940' fumarole conduit whereas H_2 denotes the length of a low-temperature one. Then:

$$H_2 = \sqrt{80^2 \cdot 6} \cong 195 \text{ m} \tag{8}$$

These simple calculations show a slower increase in the length of gas conduits in the case of different depths of gas sources according to model 1-3 than was derived from model 1-2. This fact, however, is not in contradiction with the linear regularity of maximum fumarolic temperature distributions in the Kudriavy crater but rather testifies to an irregular shape of the apical and peripheral parts of the magmatic chamber. The length of high-temperature fumarolic conduits and the depth of the apical part of the magma chamber is estimated to be about 100 m, whereas the depth of the peripheral part with low-temperature fumarolic channels is considered to be about 200 m.

5. Conclusions

(1) The thermal budget of the fumarolic system at the Kudriavy volcano is controlled by the hydrothermal system inside the volcanic edifice. Meteoric water mass flow, boiling and admixing to fumarolic gases affect fumarolic gas temperatures and hydrogen isotope composition. The decrease in gas temperature is proportional to the quantity of admixing meteoric water when the heat of evaporation is accounted for. Magmatic gas can be cooled down by 1000°C when diluted with meteoric water by less than 50%. The extrapolation of the mixing $T–X^m$ trend to the magmatic end-member allowed an estimation of magma temperature of about 1050°C.

(2) Low-temperature fumaroles at Kudriavy may be thermally buffered by the boiling processes of meteoric waters in the mixing zone at pressures of 3–12 bar. If the zone of meteoric water boiling and mixing is localized at some depth in the volcano structure then these values may reflect the hydrostatic pressures of water columns about 30–120 m in height from the level of underground waters and hence the depths of the mixing/boiling zone. In contrast, if this zone is distributed along the length of fumarolic conduits then those pres-

sure values will correspond to some average pressures of meteoric water boiling and admixing.

(3) Conductive heat transfer is governed by conductive heat exchange between gases and country rocks and appears to be responsible for the temperature distribution around the local fumaroles, whereas convective heat transfer in the hydrothermal system controls the maximum temperatures of the fumaroles and the temperature distribution inside the fumarolic fields. In the case of Kudriavy, the conductive temperature gradient in country rocks around fumaroles reaches values of about 140°C/m. The temperature distribution within the fumarolic areas is about 10°C/m. These data explain the occurrence of fumaroles with a wide temperature range up to 800°C at the same fumarolic field.

(4) The process of adiabatic gas expansion is expected to be very efficient in the fumarolic system of Kudriavy. Very high temperatures of surface fumaroles imply that the pressure difference between the magmatic gas source and the surface is not larger than 2–3 bar when adiabatic gas expansion is accounted for.

(5) The length of the 'main' fumarolic gas conduit of about 80 m is estimated from the linear correlation between maximum temperatures of fumarolic fields and distances to the highest-temperature 'F-940' fumarole. This value may correspond to the depth of the apical part of the magmatic chamber.

(6) The significant variations in the degree of meteoric water admixing to low- and high-temperature fumaroles suggest different lengths of gas conduits. It is likely that different fumarolic fields have different depths of gas sources within a single magmatic chamber. In this case, the linear regularity of the maximum fumarolic temperature distribution at Kudriavy crater suggests an irregular shape of the apical and peripheral parts of the magmatic chamber. The possible length of low-temperature fumarolic channels at the periphery of the magmatic chamber is estimated to be about 200 m.

References

Botcharnikov, R.E., 2002. Physical and Chemical Aspects of Magma Degassing at Kudriavy Volcano, Kurile Islands. PhD Thesis, 175 pp. (in Russian).

Botcharnikov, R.E., Knyazik, V.A., Steinberg, A.S., Steinberg, G.S., 1998. The emission of gases and petrogenetic and ore elements in the Kudryavyi volcano on Iturup Island, the Kuriles. Trans. Russ. Acad. Sci. 361, 858–861.

Capasso, G., Favara, R., Inguaggiato, S., 2000. Interaction between fumarolic gases and thermal groundwaters at Vulcano Island (Italy): evidences from chemical composition of dissolved gases in waters. J. Volcanol. Geotherm. Res. 102, 309–318.

Carrigan, C.R., 1986. A two-phase hydrothermal cooling model for shallow intrusions. J. Volcanol. Geotherm. Res. 28, 175–192.

Cathles, L.M., 1977. An analysis of the cooling of intrusives by ground-water convection which includes boiling. Chem. Geol. 72, 804–826.

Chiodini, G., Cioni, R., Marini, L., 1993. Reactions governing the chemistry of crater fumaroles from Vulcano Island, Italy, and implications for volcanic surveillance. Appl. Geochem. 8, 357–371.

Chiodini, G., Allard, P., Caliro, S., Parello, F., 2000. ^{18}O exchange between steam and carbon dioxide in volcanic and hydrothermal gases: Implications for the source of water. Geochim. Cosmochim. Acta 64, 2479–2488.

Connor, C.B., Clement, B.M., Song, X., Lane, S.B., West-Thomas, J., 1993. Continuous monitoring of high-temperature fumaroles on an active lava dome, volcan Colima, Mexico: Evidence of mass flow variation in response to atmospheric forcing. J. Geophys. Res. 98, 19,713–19,722.

Criss, E.R., Taylor, H.P., 1986. Meteoric-hydrothermal systems. In: Valley, J.W., Taylor, H.P. Jr., O'Neil, J.R.

(Eds.), Stable Isotopes in High Temperature Geological Processes. Rev. Mineral. 16, 373–424.

Dobson, P.F., Epstein, S., Stolper, E.M., 1989. Hydrogen isotope fractionation between coexisting vapor and silicate glasses and melts at low pressure. Geochim. Cosmochim. Acta 53, 2723–2730.

Ermakov, V.A., Semakin, V.P., 1996. Geology of caldera Medvezhya (Iturup, Kuril Islands). Trans. Russ. Acad. Sci. 351, 361–365.

Ermakov, V.A., Steinberg, G.S., 1999. Kudryavyi volcano and evolution of Medvezhiya caldera (Iturup Il., Kuril Ils.) (in Russian). Volcanol. Seismol. 3, 19–40.

Fischer, T.P., Sturchio, N.C., Stix, J., Arehart, G.B., Counce, D., Williams, S.N., 1997. The chemical and isotopic composition of fumarolic gases and spring discharges from Galeras Volcano, Colombia. J. Volcanol. Geotherm. Res. 77, 229–253.

Fischer, T.P., Giggenbach, W.F., Sano, Y., Williams, S.N., 1998. Fluxes and sources of volatiles discharged from Kudryavy, a subduction zone volcano, Kurile Islands. Earth Planet. Sci. Lett. 160, 81–96.

Giggenbach, W.F., 1987. Redox processes governing the chemistry of fumarolic gas discharges from White Island, New Zealand. Appl. Geochem. 2, 143–161.

Giggenbach, W.F., 1992a. Isotopic shifts in waters from geothermal and volcanic systems along convergent plate boundaries and their origin. Earth Planet. Sci. Lett. 113, 495–510.

Giggenbach, W.F., 1992b. The compositions of gases in geothermal and volcanic systems as a function of tectonic setting. Proc. Int. Symp. Water-Rock Interact. 8, 873–878.

Giggenbach, W.F., 1996. Chemical composition of volcanic gases. In: Scarpa, Tilling (Eds.), Monitoring and Mitigation of Volcanic Hazards. Springer, Berlin, pp. 221–256.

Giggenbach, W.F., Sheppard, D.S., 1989. Variations in the temperature and chemistry of White Island fumarole discharges 1972–1985. In: Houghton, B.F., Nairn, I.A. (Eds.), The 1976–82 Eruption Sequence at White Island Volcano (Whakaari), Bay of Plenty, New Zealand. NZ Geol. Surv. Bull. 103, 119–126.

Goff, F., McMurtry, G.M., 2000. Tritium and stable isotopes of magmatic waters. J. Volcanol. Geotherm. Res. 97, 347–396.

Gorshkov, G.S., 1970. Volcanism and Upper Mantle: Investigation in Kurile Island Arc System. Plenum Press, London.

Haar, L., Gallagher, J.S., Kell, G.S., 1984. NBS/NRC Steam Tables: Thermodynamic and Transport Properties and Computer Programs for Vapor and Liquid States of Water in SI Units. Hemisphere, Washington, DC, 312 pp.

Hardee, H.C., 1982. Permeable convection above magma bodies. Tectonophysics 84, 179–195.

Isachenko, V.P., Osipova, V.A., Sukomel, A.S., 1969. Heat transfer (cover to cover translation). Energia, Moscow, 440 pp. (in Russian).

Korzhinsky, M.A., Tkachenko, S.I., Botcharnikov, R.E., Zhdanov, N.N., Osadchii, E.G., 2000. Sensor equipment for measuring the parameters and composition of volcanic gases. Results of measurements at Kudriavy volcano, South Kuriles. In: VIIth Workshop on Chemistry of Volcanic Gases, Kyushu, Japan (abstract).

Korzhinsky, M.A., Botcharnikov, R.E., Tkachenko, S.I., Steinberg, G.S., 2002. Decade-long study of degassing at Kudriavy volcano, Iturup, Kurile Islands (1990–1999): Gas temperature and composition variations, and occurrence of 1999 phreatic eruption. Earth Planets Space 54, 337–347.

Le Guern, F., 1987. Mechanism of energy transfer in the lava lake of Niragongo (Zaire), 1959–1977. J. Volcanol. Geotherm. Res. 31, 17–31.

Le Guern, F., Carbonnelle, J., Tazieff, H., 1979. Erta'Ale lava lake: Heat and gas transfer to the atmosphere. J. Volcanol. Geotherm. Res. 6, 27–48.

Matsuhisa, Y., 1992. Origin of magmatic waters in subduction zones: stable isotope constraints. Rep. Geol. Surv. Jpn. 279, 104–109.

Matsuo, S., Suzuoki, T., Kusakabe, M., Wada, H., Suzuki, M., 1974. Isotopic and chemical composition of volcanic gases from Satsuma-Iwojima, Japan. Geochem. J. 8, 165–173.

McGetchin, T.R., Chouet, B.A., 1979. Energy budget of the volcano Stromboli, Italy. Geophys. Res. Lett. 6, 317–320.

Mizutani, Y., 1978. Isotopic compositions of volcanic steam from Showashinzan Volcano, Hokkaido, Japan. Geochem. J. 12, 57–63.

Mizutani, Y., Sigiura, T., 1982. Variations in chemical and isotopic compositions of fumarolic gases from Showashinzan volcano, Hokkaido. Japan. Geochem. J. 16, 63–71.

Murphy, M.D., Sparks, R.S.J., Barclay, J., Carroll, M.R., Lejeune, A-M., Brewer, T.S., Macdonald, R., Black, S., Young, S., 1998. The role of magma mixing in triggering the current eruption at the Soufriere Hills volcano, Montserrat, West Indies. Geophys. Res. Lett. 25, 3433–3436.

Nakagawa, M., Wada, K., Thordarson, T., Wood, C.P., Gamble, J.A., 1999. Petrologic investigations of the 1995 and 1996 eruptions of Ruapehu volcano, New Zealand: formation of discrete and small magma pockets and their intermittent discharge. Bull. Volcanol. 61, 15–31.

Nuccio, P.M., Paonita, A., Sortino, F., 1999. Geochemical modeling of mixing between magmatic and hydrothermal gases: the case of Volcano Island, Italy. Earth Planet. Sci. Lett. 167, 321–333.

Ohminato, T., Erditato, D., 1997. Broadband seismic observation at Satsuma-Iwojima, Japan. Geophys. Res. Lett. 24, 2845–2848.

O'Neil, J.R., 1986. Theoretical and experimental aspects of isotopic fractionation. In: Valley, J.W., Taylor, H.P. Jr., O'Neil, J.R. (Eds.), Stable Isotopes in High Temperature Geological Processes. Rev. Mineral. 16, 1–40.

Paonita, A., Favara, R., Nuccio, P.M., Sortino, F., 2002. Genesis of fumarolic emissions as inferred by isotope mass balances: CO_2 and water at Vulcano Island, Italy. Geochim. Cosmochim. Acta 66, 759–772.

Pineau, F., Shilobreeva, S., Kadik, A.A., Javoy, M., 1998. Water solubility and D/H fractionation in the system ande-

sibasalt-H_2O at 1250°C and between 0.5 and 3 kbars. Chem. Geol. 147, 173–184.

Piskunov, B.N., Rybin, A.V., Sergeev, K.F., 1999. Petrogeochemical characteristics of rocks from the Medvezh'ya caldera, the Iturup Island, Kuril Islands. Trans. Russ. Acad. Sci. 368, 989.

Richet, P., Bottinga, Y., Javoy, M., 1977. A review of H, C, N, O, S, and Cl stable isotope fractionation among gaseous molecules. Annu. Rev. Earth Planet. Sci. 5, 65–110.

Rowe, G.L., Brantley, S.L., Fernandez, M., Fernandez, J.F., Borgia, A., Barquero, J., 1992. Fluid-volcano interaction in an active stratovolcano: the crater lake system of Poas volcano, Costa Rica. J. Volcanol. Geotherm. Res. 49, 23–51.

Shevenell, L., 1991. Tritium in thermal waters discharging in Loowit Canyon, Mount St. Helens, Washington, USA. Chem. Geol. 94, 123–135.

Shevenell, L., Goff, F., 2000. Temporal geochemical variations in volatile emissions from Mount St. Helens, USA, 1980–1994. J. Volcanol. Geotherm. Res. 99, 123–138.

Shinohara, H., Giggenbach, W.F., Kazahaya, K., Hedenquist, J.W., 1993. Geochemistry of volcanic gases and hot springs of Satsuma-Iwojima, Japan: Following Matsuo. Geochem. J. 27, 271–285.

Shinohara, H., Kazahaya, K., Saito, G., Matsushima, N., Kawanabe, Y., 2002. Degassing activity from Iwodake rhyolitic cone, Satsuma-Iwojima volcano, Japan: Formation of a new degassing vent. Earth Planets Space 54, 175–185.

Simakin, A.G., Botcharnikov, R.E., 2001. Effects of compositional convection at degassing of stratified magma. J. Volcanol. Geotherm. Res. 105, 207–224.

Simkin, T., Siebert, L., 1994. Volcanoes of the World, 2nd edn. Smithsonian Institution Geoscience Press, Washington, DC, 349 pp.

Stevenson, D.S., 1993. Physical models of fumarolic flow. J. Volcanol. Geotherm. Res. 57, 139–156.

Sudo, Y., Hurst, A.W., 1998. Temperature changes at depths to 150 metres near the active crater of Aso Volcano: preliminary analysis of seasonal and volcanic effects. J. Volcanol. Geotherm. Res. 81, 159–172.

Symonds, R.B., Mizutani, Y., Briggs, P.H., 1996. Long-term geochemical surveillance of fumaroles at Showa-Shinzan dome, Usu volcano, Japan. J. Volcanol. Geotherm. Res. 73, 177–211.

Taran, Yu.A., Pilipenko, V.P., Rozhkov, A.M., Vakin, E.A., 1992. A geochemical model for fumaroles of the Mutnovsky volcano, Kamchatka, USSR. J. Volcanol. Geotherm. Res. 49, 269–283.

Taran, Yu.A., Hedenquist, J.F., Korzhinsky, M.A., Tkachenko, S.I., Shmulovich, K.I., 1995. Geochemistry of magmatic gases from Kudryavy volcano, Iturup, Kuril islands. Geochim. Cosmochim. Acta 59, 1749–1761.

Taran, Y.A., Bernard, A., Gavilanes, J.-C., Lunezheva, E., Cortes, A., Armienta, M.A., 2001. Chemistry and mineralogy of high-temperature gas discharges from Colima volcano, Mexico. Implications for magmatic gas-atmosphere interaction. J. Volcanol. Geotherm. Res. 108, 245–264.

Tedesco, D., Scarsi, P., 1999. Chemical (He, H_2, CH_4, Ne, Ar, N_2) and isotopic (He, Ne, Ar, C) variations at the Solfatara crater (southern Italy): mixing of different sources in relation to seismic activity. Earth Planet. Sci. Lett. 171, 465–480.

Tkachenko, S.I., 1996. High-temperature Fumarolic Gases, Condensates and Sublimates of Kudriavy Volcano, Iturup Island, Kurile Islands. PhD Thesis, Moscow.

Tkachenko, S.I., Korzhinsky, M.A., Taran, Yu.A., Pokrovsky, B.G., Steinberg, G.S., Shmulovich, K.I., 1992. Gas jets of Kudriavy volcano, Iturup Island, Kuriles. Trans. Russ. Acad. Sci. 333, 227–230.

Todesco, M., 1997. Origin of fumarolic fluids at Volcano (Italy). Insights from isotope data and numerical modeling of hydrothermal circulation. J. Volcanol. Geotherm. Res. 79, 63–85.

Truesdell, A.H., White, D.E., 1973. Production of superheated steam from vapor-dominated geothermal reservoirs. Geothermics 2, 154–173.

Venezhky, D.Y., Rutherford, M.J., 1999. Petrology and Fe-Ti oxide reequilibration of the 1991 Mount Unzen mixed magma. J. Volcanol. Geotherm. Res. 89, 213–230.

Vlasov, G.M., Petrachenko, E.D., 1971. In: Volcanic Sulfur Ore Deposits and Some Problems of Hydrothermal Ore Formation. Nauka, Moscow, 360 pp. (in Russian).

Vukalovich, M.P., Novikov, I.I., 1972. Thermodynamics. Mashinostroenie, Moscow, 672 pp. (in Russian).

Wahrenberger, C.M., 1997. Some Aspects of the Chemistry of Volcanic Gases. Ph.D. Dissertation, Zurich.

Zimmer, M., Erzinger, J., Sulistiyo, Y., 2000. Continuous gas monitoring with a chromatograph and an alpha scintillation counter on Merapi volcano, Indonesia. In: Proceedings VIIth Field Workshop on Volcanic Gases, Satsuma Iwojima and Kuju, Japan.